10 *Acicular Ferrite*

10.1 General Characteristics and Morphology

Highly organised microstructures can often be found in steels; for example, ferrite plates frequently grow in the form of packets containing parallel plates which are in the same crystallographic orientation. This can be harmful to mechanical properties because cleavage cracks can propagate readily across the packets.

Some of the most exciting recent developments in wrought and welded steel technology have involved *acicular ferrite* (Grong and Matlock, 1986; Abson and Pargeter, 1986). Far from being organised, this microstructure is better described as chaotic. The plates of acicular ferrite nucleate heterogeneously on small nonmetallic inclusions and radiate in many different directions from these point nucleation sites (Fig. 10.1). Crystallographic data show highly misoriented plates nucleated on the same inclusion (Gourgues *et al*., 2000). Propagating cracks are then deflected on each encounter with a differently oriented acicular ferrite plate. This gives rise to superior mechanical properties, especially toughness.

Acicular ferrite is therefore widely recognised to be a desirable microstructure. This chapter deals with the mechanism by which it forms and with the role of inclusions in stimulating its formation.

The term *acicular* means shaped and pointed like a needle but this is misleading because the true shape is that of a lenticular plate. The aspect ratio of the plates has never been measured but in random planar sections, they are typically about 10 μm long and approximately 1 μm wide, so that the true aspect ratio is likely to be much smaller than 0.1.

An arc-weld deposit typically contains some $10^{18}\,m^{-3}$ inclusions of a size greater than 0.05 μm, with a mean size of about 0.4 μm, distributed throughout the microstructure. Inclusions form as oxygen in the liquid weld metal reacts with strong deoxidising elements such as silicon, aluminium and titanium. Slag-forming compounds which form a part of the system designed to protect weld metal from the environment, may also become trapped in the solid at the advancing δ-ferrite/liquid interface. Inclusions promote intragranular nucleation of acicular ferrite plates and hence improve toughness without

[13:35 3/9/01 C:/3B2 Templates/keith/3750 BAINITE.605/3750-010.3d] Ref: 0000 Auth: Title: Chapter 00 Page: 237 237-276

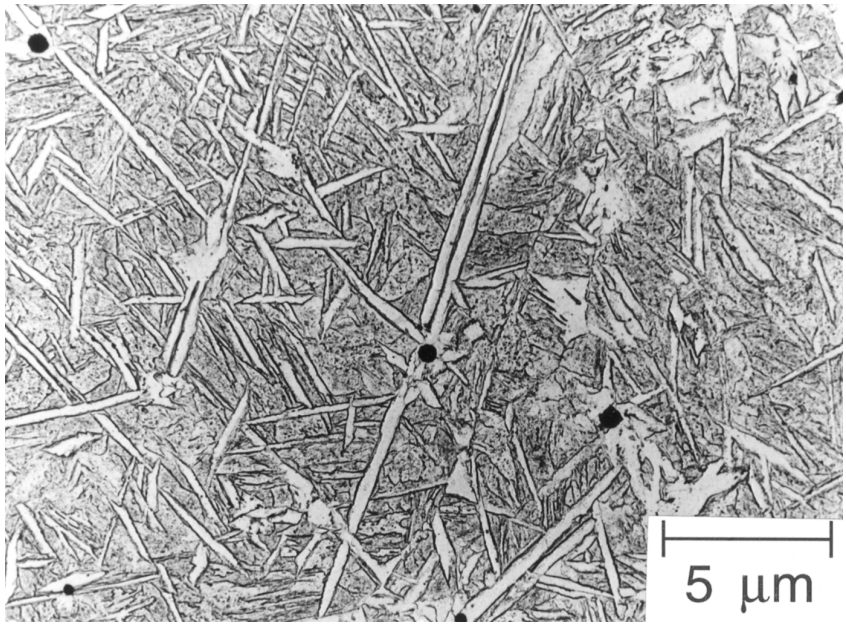

Fig. 10.1 Replica transmission electron micrograph of acicular ferrite plates in a steel weld deposit (Barritte, 1982).

compromising strength. But they also are responsible for the nucleation of voids during ductile fracture, or the nucleation of cleavage cracks during brittle fracture. Achieving a balance between these conflicting factors is the essence of good design. The inclusion microstructure is particularly important in this respect (Fig. 10.2). For example, nonmetallic particles in certain submerged arc weld deposits consist of titanium nitride cores, encapsulated in a glassy phase containing manganese, silicon and aluminium oxides, with a thin layer of manganese sulphide titanium oxide partly covering the surface of the inclusions (Barbaro *et al*., 1988). The development of this complex microstructure has been modelled using nucleation and growth theory (Babu *et al*., 1995).

Inclusions can be oxides or other compounds but the important point is that they may stimulate acicular ferrite (Ito and Nakanishi, 1976). The nucleation of a single plate on an inclusion can in turn stimulate others to nucleate autocatalytically, so that a one-to-one correspondence between the number of active inclusions and the number of acicular ferrite plates is not expected (Ricks *et al*., 1982).

The shape change accompanying the growth of acicular ferrite has been characterised qualitatively as an invariant-plane strain (Fig. 10.3). Like bainite, the shape deformation causes plastic deformation in the adjacent austenite. The

[13:36 3/9/01 C:/3B2 Templates/keith/3750 BAINITE.605/3750-010.3d] Ref: 0000 Auth: Title: Chapter 00 Page: 238 237-276

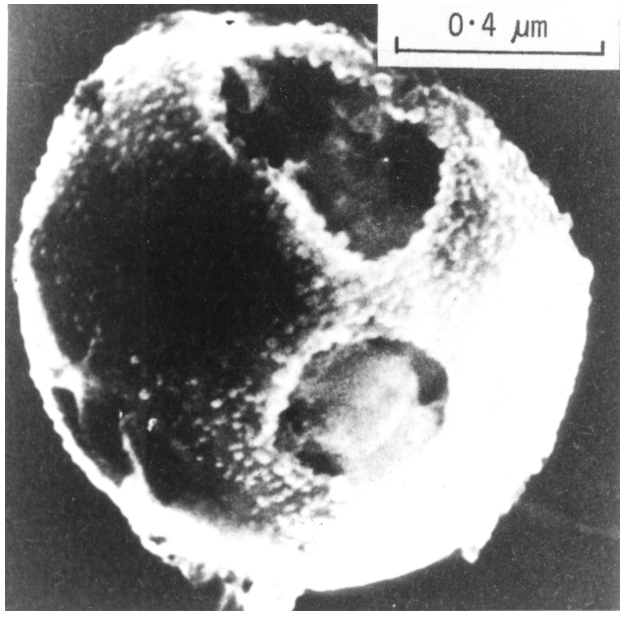

Fig. 10.2 Scanning transmission electron micrograph of a nonmetallic inclusion in a steel weld metal. The inclusion surface is very irregular, and it features many phases (after Barritte, 1982).

resulting dislocations are inherited by the acicular ferrite as it grows, giving a dislocation density which is typically at $10^{14}\,\mathrm{m}^{-2}$, and which contribute some 145 MPa to its strength. The stored energy of acicular ferrite is similar to that of bainite at about $400\,\mathrm{J\,mol}^{-1}$ (Strangwood and Bhadeshia, 1987; Yang and Bhadeshia, 1987). Consistent with the observed shape change, microanalysis experiments prove that there is no long-range partitioning of substitutional solutes during the formation of acicular ferrite (Strangwood, 1987); indeed, atomic resolution experiments have demonstrated that there is no partitioning on the finest conceivable scale (Chandrasekharaiah *et al.*, 1994).

Acicular ferrite clearly grows by a displacive mechanism so there are other consequences on the development of microstructure. Thus, plates of acicular ferrite are confined to the grains in which they grow because the coordinated movement of atoms associated with the displacive transformation mechanism cannot be sustained across grain boundaries. The α_a/γ orientation relationship is *always* found to be one in which a close-packed plane of the austenite is nearly parallel to the most densely packed plane of α_a. Corresponding close-packed directions within these planes are found to be within a few degrees of each other (Strangwood and Bhadeshia, 1987). As with bainite, the size of the acicular ferrite plates increases with transformation temperature; Horii

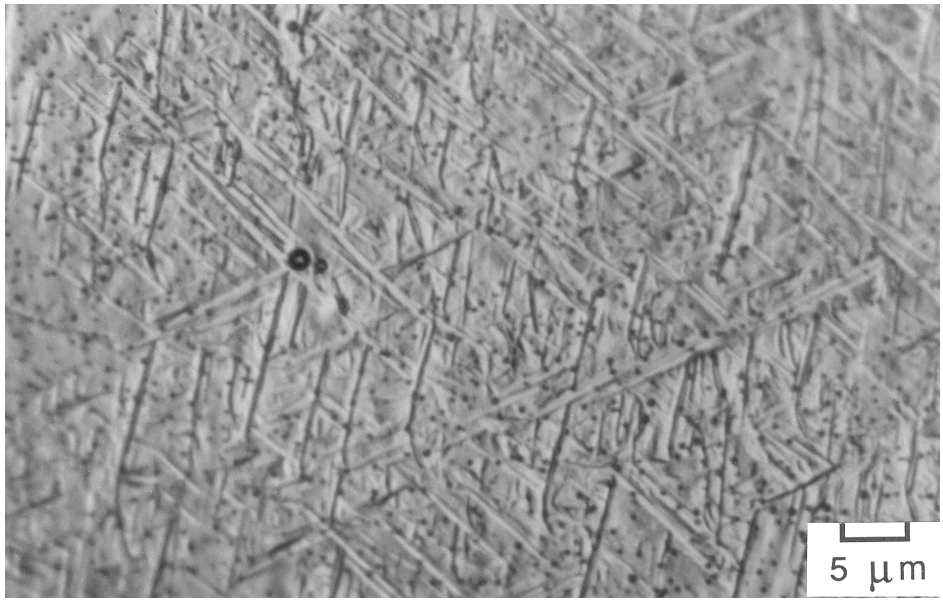

Fig. 10.3 Nomarski interference contrast micrograph illustrating the displacements associated with the formation of acicular ferrite (Strangwood and Bhadeshia, 1987).

et al.(1988) reported that the apparent plate thickness and length changed from about 1 to 2 μm as the weld cooling rate was reduced.

10.2 Mechanism of Growth

The acicular ferrite transformation exhibits the incomplete-reaction phenomenon, an important characteristic of bainite. The extent of reaction decreases towards zero as the transformation temperature is increased towards B_S (Yang and Bhadeshia, 1987; Strangwood and Bhadeshia, 1987). Isothermal transformation stops when the carbon concentration of the residual austenite exceeds the T_0' curve (Fig. 10.4). This implies that acicular ferrite grows supersaturated with carbon, but the excess carbon is shortly afterwards rejected into the remaining austenite.

Acicular ferrite is intragranularly nucleated bainite so it should be possible to switch between these two morphologies by controlling the nucleation site. A bainitic microstructure can be replaced by one containing acicular ferrite by increasing the oxygen, and hence the inclusion content (Ito *et al*., 1982). After all, the appearance of the acicular ferrite microstructure is only different from

[13:36 3/9/01 C:/3B2 Templates/keith/3750 BAINITE.605/3750-010.3d] Ref: 0000 Auth: Title: Chapter 00 Page: 240 237-276

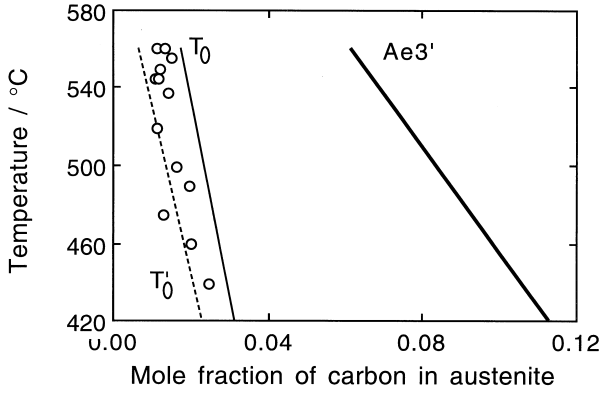

Fig. 10.4 Data from experiments in which the austenite is transformed isothermally to acicular ferrite, showing that the reaction stops when the carbon concentration of the austenite reaches the T_0' curve (Strangwood and Bhadeshia, 1987).

that of bainite because it nucleates intragranularly in steels containing a greater number density of inclusions than austenite grain surface nucleation sites (Yang and Bhadeshia, 1986). Acicular ferrite does not grow in sheaves because their development is stifled by impingement between plates nucleated independently at adjacent sites. Indeed, both microstructures can be obtained under identical isothermal transformation conditions in the same inclusion-containing steel. Bainite forms when the austenite grain size is small because nucleation then predominates at the grain boundaries. Subsequent growth then swamps the interiors of the austenite grains, preventing the development of acicular ferrite. When the austenite grain size is large, the number density of inclusions becomes large relative to boundary nucleation sites promoting the formation of acicular ferrite at the expense of bainite (Fig. 10.5).

This basic theory explains many observations on welds where the heat due to welds produces a gradient of austenite grain size in the heat affected zone (HAZ), with the largest grains adjacent to the fusion surface. When steels containing appropriate inclusions are welded, the ratio of acicular ferrite to bainite is the highest in the HAZ nearest the fusion boundary where the austenite grain size is at a maximum (Fig. 10.6a). In the absence of inclusions, the acicular ferrite content is always very small, Fig. 10.6b (e.g. Imagumbai *et al.*, 1985).

In another supporting experiment, Harrison and Farrar (1981) removed the inclusions by vacuum remelting a weld; when cooled, the steel transformed into bainite instead of the original acicular ferrite microstructure.

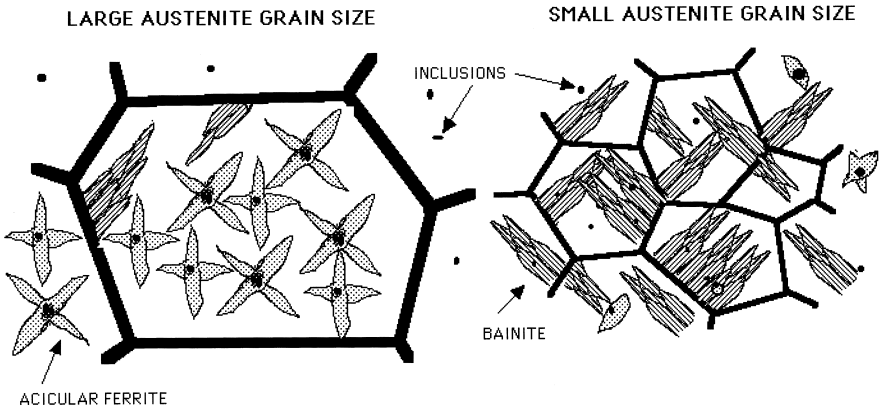

Fig. 10.5 The effect of austenite grain size on the development of microstructure in an inclusion-containing steel. A small grain sized sample has a relatively large number density of grain boundary nucleation sites so bainite dominates the microstructure, whereas a relatively large number density of intragranular nucleation sites leads to a microstructure consisting predominantly of acicular ferrite.

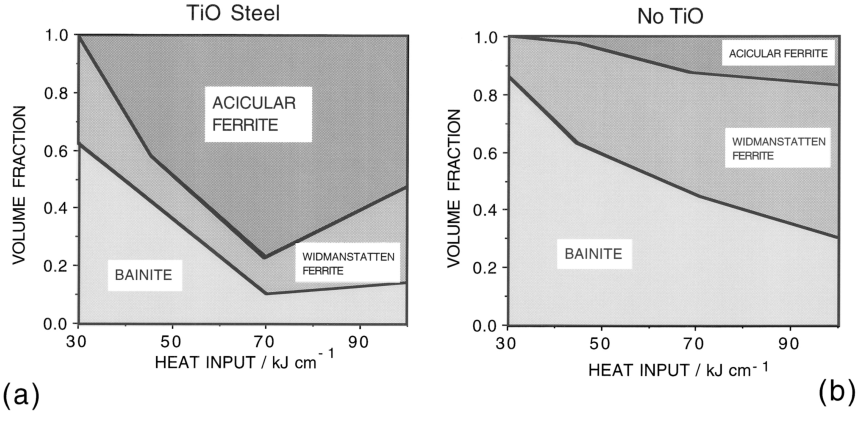

Fig. 10.6 Changes in the microstructure of the heat affected zone of welds, as a function of the heat input during welding: (a) steel containing titanium oxide particles; (b) ordinary steel without inclusion inoculation (after Chijiiwa *et al*., 1988).

We have emphasised that the transformation mechanism for acicular ferrite is identical to that for bainite. However, all phases can nucleate on inclusions, including Widmanstätten ferrite (Dubé, 1948; Ali and Bhadeshia, 1991). Thewlis *et al*. (1997) have argued that in some welds the so-called acicular

[13:36 3/9/01 C:/3B2 Templates/keith/3750 BAINITE.605/3750-010.3d] Ref: 0000 Auth: Title: Chapter 00 Page: 242 237-276

ferrite may predominantly be intragranularly nucleated Widmanstätten ferrite rather than bainite. They reached this conclusion by noting that the estimated bainite-start (B_S) temperature was lower than that at which coarse plates nucleated on very large inclusions (3–9 μm diameter). Although there is uncertainty in their calculated B_S values, the conclusion that a mixed microstructure of intragranularly nucleated Widmanstätten ferrite and intragranularly nucleated bainite (i.e. acicular ferrite) was obtained seems justified. Intragranularly nucleated Widmanstätten ferrite can be distinguished readily from bainite by the scale of the optical microstructure.

Widmanstätten ferrite plates are always much coarser than bainite because what appears as a single plate using optical microscopy is in fact a pair of self accommodating plates. The shape deformation consists of two adjacent invariant-plane strains which mutually accommodate and hence reduce the strain energy, thus allowing the plates to be coarse (Bhadeshia, 1981a).

Acicular ferrite is sometimes considered to be intragranularly nucleated Widmanstätten ferrite on the basis of the observation of 'steps' at the transformation interface, which are taken to imply a ledge growth mechanism (Ricks *et al*., 1982). The step mechanism of interfacial motion does not necessarily indicate the mechanism of *transformation*. The observations are in any case weak; perturbations of various kinds can always be seen on transformation interfaces between ferrite and austenite. Such perturbations do not, however, necessarily imply a step mechanism of growth. Evidence that the residual austenite is enriched in carbon is sometimes quoted in support of the contention that α_a is Widmanstätten ferrite but as pointed out above, the enrichment can occur during or after the transformation event.

The weight of the evidence is that the acicular ferrite recognised in most weld microstructures is intragranularly nucleated bainite. And that the term acicular ferrite should be reserved for this fine microstructure. If coarse Widmanstätten ferrite forms on inclusions then it can be called 'intragranularly nucleated Widmanstätten ferrite'. The names given to phases are important because they imply a mechanism of transformation which can be used in theoretical models. It is particularly important to avoid naming mixtures of microstructures.

10.3 Mechanism of Nucleation

A popular treatment of acicular ferrite nucleation based on classical heterophase fluctuation theory is due to Ricks *et al*. (1981,1982). It relies on the occurrence of chance fluctuations in crystal structure. The activation energy (G^*) for a fluctuation which is large enough to stimulate critical nucleus depends on the inverse square of the chemical driving force $G^* \propto \Delta G^{-2}$ (Chapter 6). With this theory it is possible to explain why larger spherical non-metallic inclusions are

more effective for heterogeneous nucleation. An embryo which forms in contact with the surface will have a smaller curvature and a corresponding smaller surface-to-volume ratio when the inclusion is large. A flat austenite grain surface is therefore expected to be a more potent heterogeneous nucleation site than a spherical inclusion. Furthermore, the energy of the interface between the ferrite and the inclusion is likely to be larger relative to the case when ferrite nucleates on austenite grain surfaces. It follows that the activation energy for nucleation on an inclusion, relative to that for nucleation on an austenite grain surface should vary as illustrated in Fig. 10.7.

An alternative interpretation uses the bainite nucleation theory discussed in Chapter 6. Nucleation is said to occur when an appropriate array of dislocations is able to dissociate rapidly. The activation energy is that for the migration of the embryo/austenite interface; it decreases linearly as the driving force increases. The driving force must be calculated to allow for the diffusion of carbon although the overall mechanism of nucleation remains displacive since the dislocation array considered is glissile.

It follows that the driving force available for nucleation at the highest temperature at which transformation occurs (T_h) should be proportional to T_h (Chapter 6). This is found to be the case as illustrated in Fig. 10.8, which is comparable to Fig. 6.4a. The line is identified with the universal nucleation

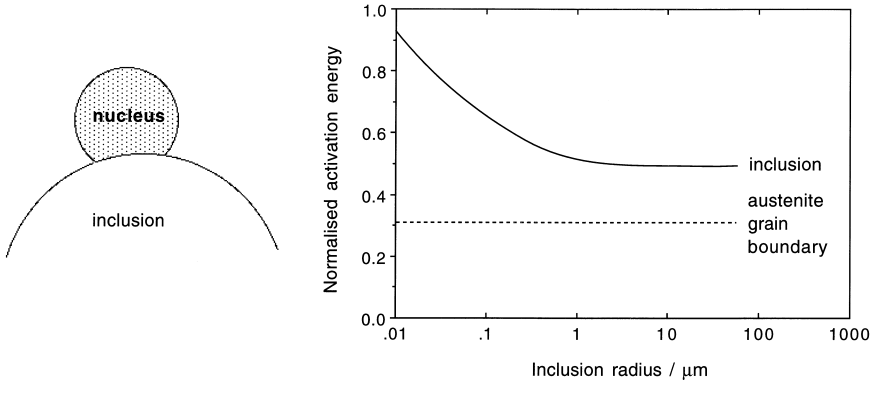

Fig. 10.7 The formation of a truncated spherical nucleus on a spherical inclusion. The activation energy for nucleation has been normalised with respect to that for homogeneous nucleation. The calculations assume that the interfacial energy between austenite and ferrite is the same as that for an austenite grain boundary; that the inclusion/ferrite and inclusion/austenite interface energies are identical and that these are both greater than an austenite grain boundary energy. After Ricks *et al*. (1981, 1982).

function G_N that can be used to estimate the acicular ferrite start-temperature for any alloy.

The experiments shown in Fig. 10.8 included both bainite and acicular ferrite, the change in microstructure being achieved by controlling the austenite grain size. It is evident that both bainite and acicular ferrite can be represented by the same line, emphasising the conclusion that acicular ferrite is simply intragranularly nucleated bainite.

The displacive mechanism of nucleation relies on the existence of arrays of dislocations. It is conceivable that such arrays are generated in the proximity of non-metallic inclusions due to stresses caused by differential thermal expansion. Such stresses are more difficult to accommodate for larger inclusions, making large inclusions more potent nucleation sites. Arrays of dislocations are readily found at grain boundaries, accounting for the observation that austenite grain surfaces are most effective as nucleation sites.

10.4 Nucleation and The Role of Inclusions

Non-metallic inclusions in steels have complex multiphase microstructures which make controlled experiments designed to reveal nucleation phenomena rather difficult. A popular idea is that the most potent nucleants have a good *lattice match* with ferrite. There may then exist reproducible orientation relationships between inclusions and the ferrite plates that they nucleate (Mills *et al.*, 1987). The lattice matching is expressed as a mean percentage planar misfit κ (Bramfitt, 1970). Suppose that the inclusion is faceted on $(h\,k\,l)_I$ and

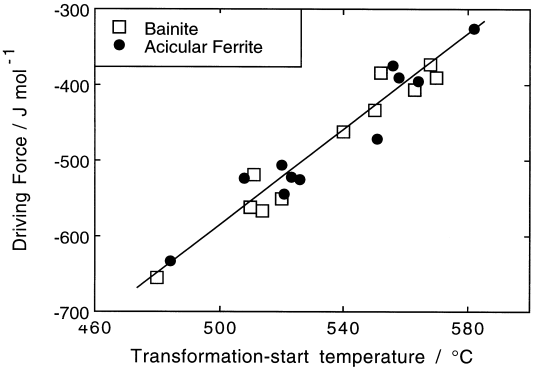

Fig. 10.8 Plot of the driving force available for the nucleation of bainite or acicular ferrite at the temperature T_h, versus T_h for a series of welding alloys. Note that each pair of bainite and acicular ferrite points represents a different alloy. After Rees and Bhadeshia, 1994.

that the ferrite deposits epitaxially with $(h\,k\,l)_\alpha \| (h\,k\,l)_I$, with a pair of corresponding rational directions $[u\,v\,w]_I$ and $[u\,v\,w]_\alpha$ inclined at an angle ϕ to each other. The interatomic spacings d along three such directions within the plane of epitaxy are examined to obtain:

$$\kappa = \frac{100}{3} \sum_{j=1}^{3} \frac{|d_j^I \cos\phi - d_j^\alpha|}{d_j^\alpha} \tag{10.1}$$

Data calculated in this manner, for a variety of inclusion phases, are presented in Table 10.1. A description of the relationship between two crystals with cubic lattices requires five degrees of freedom, three of which are needed to specify the relative orientation relationship, and a further two in order to identify the plane of contact between the two crystals. Mills *et al*. considered nine different kinds of epitaxy, confined to planes of low crystallographic indices: $\{0\,0\,1\}$, $\{0\,1\,1\}$ & $\{1\,1\,1\}$. The orientation relationships considered are listed in Table 10.1: the Bain orientation implies $\{1\,0\,0\}_\alpha \| \{1\,0\,0\}_I$ and $< 1\,0\,0 >_\alpha \| < 0\,1\,1 >_I$. The Cube orientation occurs when the cell edges of the two crystals are parallel.

Table 10.1 Misfit values between different substrates and ferrite. The data are from a more detailed set published by Mills *et al.* (1987) and include all cases where the misfit is found to be less than 5%. The inclusions all have a cubic-F lattice; the ferrite is body-centred cubic (cubic-I).

Inclusion	Orientation	Plane of Epitaxy	Misfit %
TiO	Bain	{1 0 0}	3.0
TiN	Bain	{1 0 0}	4.6
γ-alumina	Bain	{1 0 0}	3.2
Galaxite	Bain	{1 0 0}	1.8
CuS	Cube	{1 1 1}	2.8

A comparison with experiments requires not only the right orientation relationship, but the inclusion must also be faceted on the appropriate plane of epitaxy. Experiments, however, demonstrate that the ferrite/inclusion orientation relationship tends to be random (Dowling *et al*., 1986). The inclusions, which form in liquid steel, are randomly orientated but there is a fixed α_a/γ orientation so it follows that the inclusion/ferrite orientation relation must be random (Fig. 10.9). A contrary view is due to Kluken *et al*. (1991), who claim that the δ-ferrite grains sometimes nucleate on inclusions in the melt. The

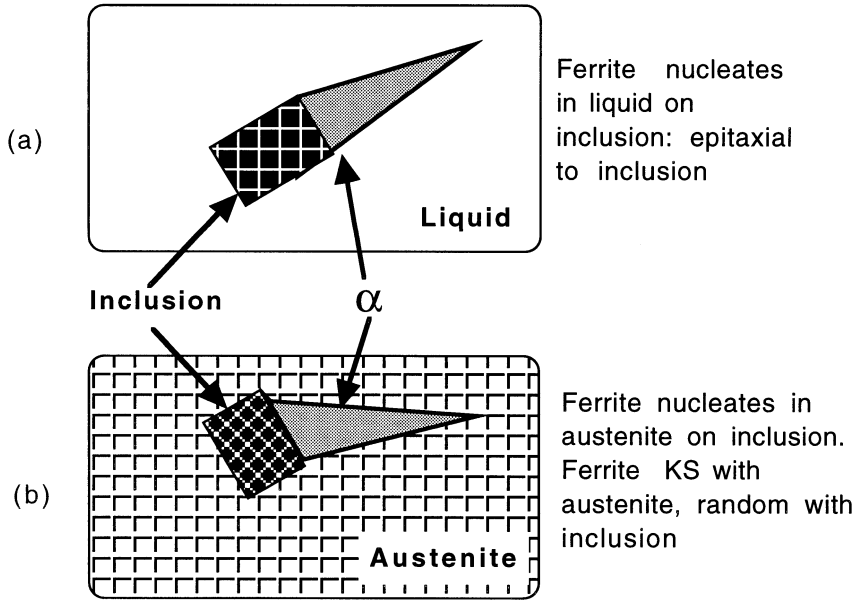

Fig. 10.9 Illustration of the orientation relationship that might develop between acicular ferrite and an inclusion. (a) When ferrite nucleates on an inclusion, with both phases surrounded by liquid; it is possible for the ferrite to adopt a favoured relationship to the inclusion since it is not limited by the liquid. (b) The inclusion, which grows from liquid, is randomly orientated to the austenite. The acicular ferrite, which has fixed orientation relationship with the austenite, must therefore be randomly orientated to the inclusion.

acicular ferrite should then bear an orientation relationship with the inclusions since it will be related to the δ-ferrite via the austenite. Textural measurements have been cited in support of this hypothesis.

Other ways in which inclusions may assist nucleation include stimulation by thermal strains, chemical heterogeneities in the vicinity of the inclusion/matrix interface; alternatively, they may simply be inert sites for heterogeneous nucleation. Pressure bonded ceramic–steel composites have been studied to reveal the potency of pure ceramic phases in stimulating the nucleation of bainite, Table 10.2 (Strangwood and Bhadeshia, 1988; Gregg and Bhadeshia, 1994a,b). A rather simple model emerges from these experiments, that those ceramics which chemically interact with the adjacent steel are most effective in nucleating bainite. A significant exception is TiO, which remains inert and yet enhances bainite formation.

There is clear evidence from the bond experiments that some minerals act as sources of oxygen which cause the steel in their vicinity to decarburise, which

[13:36 3/9/01 C:/3B2 Templates/keith/3750 BAINITE.605/3750-010.3d] Ref: 0000 Auth: Title: Chapter 00 Page: 247 237-276

Table 10.2 List of ceramics found to be chemically active in experiments designed to test for ferrite nucleation at ceramic/steel bonds.

Chemically Active	Chemically Inactive
TiO_2	TiO, Ti_2O_3, TiC, TiB_2, TiN
$Al_2Si_2O_7$	Al_2O_3
MnO_2	MnO
SiC, Si	Si_3N_4, SiO_2
CoO, V_2O_5	ZrO_2, FeS, Y_2O_3

in turn stimulates the nucleation of bainite. One such mineral is TiO_2. Structural and behavioural analogues of TiO_2 (SnO_2, MnO_2 and PbO_2) are also found to stimulate bainite in the same manner. TiO_2 and related minerals tend to form oxygen vacancy defects at elevated temperatures, thus releasing oxygen, which can penetrate the adjacent steel. On this hypothesis, all oxygen producing minerals would be expected to react with the steel, and enhance bainite formation, while non-oxygen producing minerals would not. This contrast in nucleation potential due to differences in the ability to release oxygen is illustrated by examining the nucleation potency of the perovskite structural group of ceramics. *Normal* perovskites (ABO_3 type) are structurally similar to *defect* perovskites (BO_3 type) but the ability of defect perovskites to produce oxygen is much greater. Therefore, WO_3, which is a defect perovskite is effective in nucleating bainite whereas the normal perovskite $CaTiO_3$ is found to be ineffective. Indeed, any oxygen source, for example KNO_3, is found to be effective in stimulating the nucleation of bainite.

Neither Ti_2O_3 nor TiO are oxygen sources but nevertheless stimulate bainite. Ti_2O_3 does this by absorbing manganese and hence causing a dramatic depletion in the manganese concentration in the adjacent steel. Since manganese stabilises austenite, its depletion stimulates bainite formation. By contrast, TiO remains completely inert so the mechanism by which it stimulates nucleation is not clear. It could be argued that it offers a good lattice match with ferrite. However, so does TiN, which is not particularly useful in nucleating bainite. The nucleation mechanisms are summarised in Table 10.3.

10.4.1 Aluminium and Titanium Oxides

There is evidence that titanium oxides (TiO, Ti_2O_3, TiO_2) are potent acicular ferrite nucleating agents whereas Al_2O_3 is not. Aluminium is a stronger oxidising agent than titanium so it is expected that alumina forms first, followed by

[13:36 3/9/01 C:/3B2 Templates/keith/3750 BAINITE.605/3750-010.3d] Ref: 0000 Auth: Title: Chapter 00 Page: 248 237-276

Table 10.3 Mineral classification according bainite nucleation potency.

Effective: oxygen sources	Effective: other mechanisms	Ineffective
TiO_2, SnO_2	Ti_2O_3	TiN, $CaTiO_3$
MnO_2, PbO_2	TiO	$SrTiO_3$, $\alpha - Al_2O_3$
WO_3, MoO_3		$\gamma - Al_2O_3$, $MnAl_2O_4$
KNO_3		NbC

titania, which can form as a coating on the alumina particles. Titanium oxide formation requires that there is excess oxygen left after the aluminium has combined with oxygen (Horii *et al*., 1986, 1988). The aluminium concentration should therefore be kept to a minimum, otherwise, titanium oxides do not form even if the steel contains a titanium addition Ringer *et al*., (1990).

Titanium nitride is an effective nucleant but is less thermodynamically stable at high temperatures when compared with Ti_2O_3.

$$Ti + O_2 \rightleftharpoons TiO_2 \quad G^O = -9.2 \times 10^5 - 50.2\,T \ \ J\,mol^{-1} \tag{10.2}$$

$$Ti + N \rightleftharpoons TiN \quad G^O = -3.4 \times 10^5 - 30.1\,T \ \ J\,mol^{-1} \tag{10.3}$$

where G^O is the standard free energy of formation (Kubaschewski and Evans, 1950). Nevertheless, titanium nitride is often the first to precipitate from the liquid phase.

Notwithstanding this anomaly, considerable progress can be made by assuming that the dissolved elements in a sequence consistent with their oxidising potential. For welds, this usually means that aluminium has the first call on the available oxygen, followed by titanium (Horii *et al*., 1988). Oxygen can be depleted from the melt by an excess of aluminium, preventing the formation of desirable titanium oxides. A minimisation of the aluminium content has the additional advantage that the total oxygen (and hence the inclusion content) can be reduced whilst keeping the same titanium oxide content. Nitrogen must be controlled to prevent the formation of titanium nitride, perhaps by adding boron as a nitrogen gettering agent. Trace elements like calcium, cerium and other rare earth elements, at the concentrations used for inclusion shape control in wrought alloys, do not influence the development of the acicular ferrite microstructure (Horii *et al*., 1986, 1988). These elements might enter the weld metal via the fused base metal, particularly during high heat input welding where dilution is exaggerated (Fig. 10.10).

Small concentrations of dissolved aluminium seem to promote Widmanstätten ferrite; the mechanism of this is effect is not understood

[13:36 3/9/01 C:/3B2 Templates/keith/3750 BAINITE.605/3750-010.3d] Ref: 0000 Auth: Title: Chapter 00 Page: 249 237-276

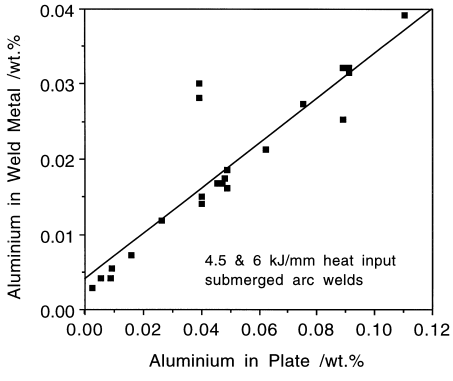

Fig. 10.10 A plot of the aluminium concentration in the weld metal versus that in the steel, illustrating the incorporation of trace elements from the base plate into the weld fusion zone during high heat input welding (Horii *et al*. 1988).

(Abson, 1987; Grong *et al*., 1988; Thewlis, 1989a,b). It may be that the presence of soluble aluminium correlates with a large overall aluminium concentration, in which case the aluminium oxide becomes γ-alumina instead of galaxite. The former is not an effective nucleant for acicular ferrite, thus allowing grain boundary nucleated Widmanstätten ferrite to grow unhindered.

The mean size of non-metallic inclusions in welds changes only a little with the aluminium concentration (Thewlis, 1989a; Evans, 1990). Although inclusions are essential for improved weld microstructure, they can also nucleate fracture. A compromise level of inclusions is required, but it seems likely most weld deposits contain more oxygen than is necessary. For example, concentrations less than 120 p.p.m. are adequate in producing an acicular ferrite microstructure in suitably alloyed wrought steels.

The character of inclusions alters with increasing aluminium concentration. The oxide particles being predominantly $MnOSiO_2$ at low Al concentrations, to be replaced by galaxite which is a mixed spinel (Al_2O_3MnO) and finally by $\gamma - Al_2O_3$ at higher aluminium concentrations (Thewlis, 1990). Galaxite has a good lattice match with ferrite and so is the desired oxide form (Table 10.1).

10.4.2 Sulphur

Manganese sulphide (MnS) particles sometimes act as heterogeneous nucleation sites. Using a steel containing 0.07 wt% of sulphur and 0.1 wt% vanadium, Ochi *et al*. (1988) produced a fine dispersion of MnS particles on which they obtained the successive precipitation of vanadium nitride, vanadium carbide and finally, idiomorphic ferrite:

[13:36 3/9/01 C:/3B2 Templates/keith/3750 BAINITE.605/3750-010.3d] Ref: 0000 Auth: Title: Chapter 00 Page: 250 237-276

$$MnS \rightarrow VN \rightarrow V_4C_3 \rightarrow \alpha_I$$

On the other hand, in more recent work, the nitride has been shown to lead directly to the nucleation of ferrite via the lattice-matching mechanism (Ishikawa *et al*., 1994).

The sulphide can itself stimulate ferrite. Thus, Yamamoto *et al*. (1987) in their titanium-containing steel, found that MnS precipitates on titanium oxides and then stimulates the nucleation of acicular ferrite. The acicular ferrite fraction decreased when the sulphur concentration was reduced to less than 0.001 wt%. However, there are contradictory results. Chijiiwa *et al*. (1988) found an increase in the acicular ferrite fraction as the sulphur concentration from was reduced from 0.005 to 0.001 wt%. Ringer *et al*. (1990) showed that Ti_2O_3 particles without any surrounding MnS films can nevertheless be effective in stimulating the intragranular nucleation of ferrite. Abson (1987) has concluded that the presence of MnS at the surface of oxide particles inhibits the nucleation of ferrite, and furthermore, that the addition of elements which getter sulphur makes the inclusions more effective.

It is therefore difficult to reach a conclusion, but it is likely that manganese sulphide can act as a substrate for the nucleation of ferrite. MnS is commonly present in commercial steels but it precipitates in the solute-enriched interdendritic regions of the solidification microstructure. These regions are rich in manganese which retards ferrite formation. Realising this, Ueshima *et al*. (1989) produced uniform distributions of MnS particles by inducing them to nucleate on oxide particles. High purity melts, each containing 0.004 wt.% of sulphur, were deoxidised using one of Al, Ti, Zr, La, Ce, Hf or Y. Of these, aluminium and titanium additions were found to be the most uniformly dispersed and insensitive to the killing time within the range 30–600s (Fig. 10.11).[†] All of the deoxidising elements studied were able to promote MnS nucleation (Fig. 10.11), but Ti_2O_3 and zirconia were particularly effective, with aluminium being the least potent in this respect. The MnS precipitated in the solid-state over a temperature range estimated to be 1050–1400°C. Whilst these results do not help resolve the role of sulphides in stimulating ferrite nucleation, they establish methods of controlling the sulphide size, distribution and precipitation. Ueshima *et al*. estimated, using diffusion theory, that the formation of MnS would lead to a manganese-depleted zone in its close proximity, a zone in which the tendency to form ferrite would be enhanced.

It is obvious that manganese depletion can only help the nucleation of ferrite. An elegant study by Mabuchi *et al*. (1996) has proved that depletion zones are

[†]During *killing*, the oxygen concentration in the molten steel is reduced by the addition of metallic elements which have a strong affinity for oxygen. The resulting oxides usually float off into the slag, although fine particles are retained. The killing time is the interval between the addition of the deoxidising element and the solidification of the steel.

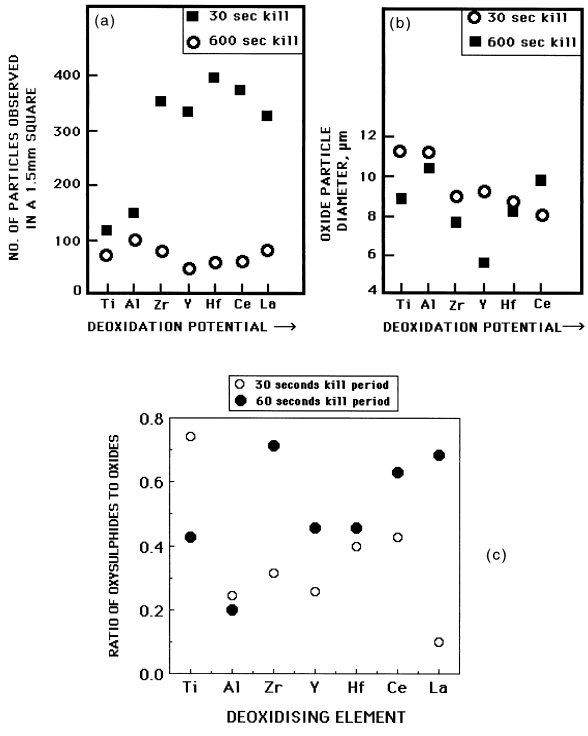

Fig. 10.11 The effects of a variety of deoxidising elements on the nature of oxide and oxysulphide precipitation in steel (Ueshima *et al*., 1989): (a) number density of oxide particles; (b) size of oxide particles; (c) propensity of the oxide to stimulate the solid-state nucleation of sulphide.

indeed to be found in the vicinity of MnS which precipitates from austenite, but the zones are rapidly homogenised soon after the precipitation is completed. The MnS is therefore only active in stimulating ferrite nucleation if the latter occurs shortly after MnS formation. Any prolonged holding in the austenite phase field homogenises the manganese concentration. For the same reason, MnS particles might be active as heterogeneous nucleation sites on the first occasion that they precipitate, but their potency is reduced if the sample is then reheated into the austenite phase field. This has significant implications for the large number of experiments based on reheated weld metals and may explain why the early results are contradictory.

10.4.3 Phosphorus

Phosphorus is another impurity element which is rarely deliberately added to steels because of its well known tendency to embrittle grain boundaries. Its concentration is usually kept below 50 p.p.m., but in welds the average

[13:36 3/9/01 C:/3B2 Templates/keith/3750 BAINITE.605/3750-010.3d] Ref: 0000 Auth: Title: Chapter 00 Page: 252 237-276

concentration can exceed 100 p.p.m. Solidification induced segregation can locally raise the concentration to 500 p.p.m. This may alter the kinetics of transformation and hence influence the development of acicular ferrite microstructure in weld deposits (Kluken and Grong, 1989b; Kluken *et al*., 1990).

The thermodynamic effect of phosphorus is to raise the Ae_3 temperature by about 460 °C per wt%, over the concentration range of interest (Bastien, 1957), although the consequences of such a big effect are not as large as might be expected (Kirkaldy *et al*., 1962).

During weld solidification, the phosphorus segregates between the δ-ferrite dendrites and cells. When solidification is complete, the δ-ferrite transforms to austenite which nucleates heterogeneously at the δ/δ grain boundaries. Kluken and Grong suggest that the austenite grain boundaries coincide with the phosphorus rich regions so this stimulates the formation of acicular ferrite; when they do not do so, ferrite plates grow from the grain boundaries and consume most of the austenite before the intragranular acicular ferrite has a chance to develop.

This hypothesis is then used to explain why the acicular ferrite content of welds decreases suddenly as the ratio of the precipitated aluminium to oxygen concentrations reaches a value of 1.13 (Fig. 10.12a). Beyond that limiting value, the nonmetallic inclusions become pure γ-alumina (Fig. 10.12b), and these apparently stimulate austenite directly from the melt. The resulting austenite

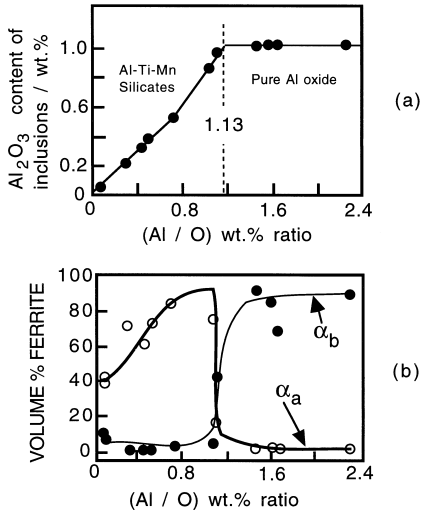

Fig. 10.12 (a) Variation in the volume fraction of acicular ferrite as a function of the precipitated-Al : oxygen ratio; (b) variation in the inclusion chemistry with the same ratio.

[13:36 3/9/01 C:/3B2 Templates/keith/3750 BAINITE.605/3750-010.3d] Ref: 0000 Auth: Title: Chapter 00 Page: 253 237-276

grain boundaries are no longer coincident with the phosphorus rich regions, thus leading to Widmanstätten ferrite formation.

These ideas are inconsistent with the fact that phosphorus increases the driving force for the transformation of austenite. A second difficulty is that in a weld, the temperature isotherms change position during cooling, so that the fastest growth direction of the austenite does not coincide with that of the δ-ferrite (Dadian, 1987).

10.4.4 Nitrogen, Titanium and Boron

Nitrogen is not often a deliberate alloying addition to steels and weld deposits. It is detrimental to the toughness even at concentrations as low as 20–120 p.p.m. The mechanism of embrittlement is strain age-hardening solid-solution hardening effects, both of which increase the yield strength and hence the ability of the material to absorb energy by plastic deformation during fracture (Lancaster, 1986; Keown *et al*., 1976; Judson and McKeown, 1982; Oldland, 1985).

Some studies suggest that nitrogen has no detectable influence on the acicular ferrite content of welds (Mori *et al*., 1981), whereas others (Okabe *et al*., 1983; Ito and Nakanishi, 1975) claim significant changes due to nitrogen. At the small concentrations of nitrogen in ferritic steels, it is unlikely that nitrogen has any significant thermodynamic effect on the $\gamma \rightarrow \alpha$ transformation. Its influence must be kinetic, perhaps via some interaction with the inclusion phases.

In practice, the effect of nitrogen in weld metals has to be considered alongside that of titanium and boron, both of which form nitrides. It appears that nitrogen, in the absence of boron, has no detectable effect on the development of microstructure (Horii *et al*., 1986, 1988; Lau *et al*., 1987, 1988). Boron is added to render austenite grain boundary nucleation sites impotent and hence to promote acicular ferrite. By contrast, nucleation at the interface between Ti_2O_3 and austenite is not retarded by boron; its diffusion into the oxide, which contains cation vacancies, leaves behind a boron-depleted zone (Yamamoto *et al*., 1996). Titanium has the function of protecting the boron from oxidation during transfer across the welding arc. It also prevents boron from combining with nitrogen to form boron nitride. Boron must be in solid solution if it is to segregate to and reduce the energy of the austenite grain surfaces, making them less effective nucleation sites.

For a given oxygen and boron concentration, the aluminium and titanium concentrations have to be large enough to getter all the available oxygen. Furthermore, there has to be enough titanium left over to combine with any nitrogen to permit boron to remain in solid solution. A method for making rational decisions during the design of titanium and boron containing deposits is illustrated in Fig. 10.13.

The assumptions involved are illustrated by the work of Kluken and Grong (1989a), whose ideas are reproduced below in an explicit formalism. The total volume fraction V_I of inclusions is approximately (Franklin, 1969):

$$V_I \simeq 0.05 w_O + 0.054(w_S - w_S^{sol}) \tag{10.4}$$

where w_i is the concentration of element i in units of weight percent and w_S^{sol} the soluble sulphur concentration, usually assumed to be about 0.003 wt%. The mass fraction of inclusions is:

$$m_I = V_I \frac{\rho_I}{\rho_S} \tag{10.5}$$

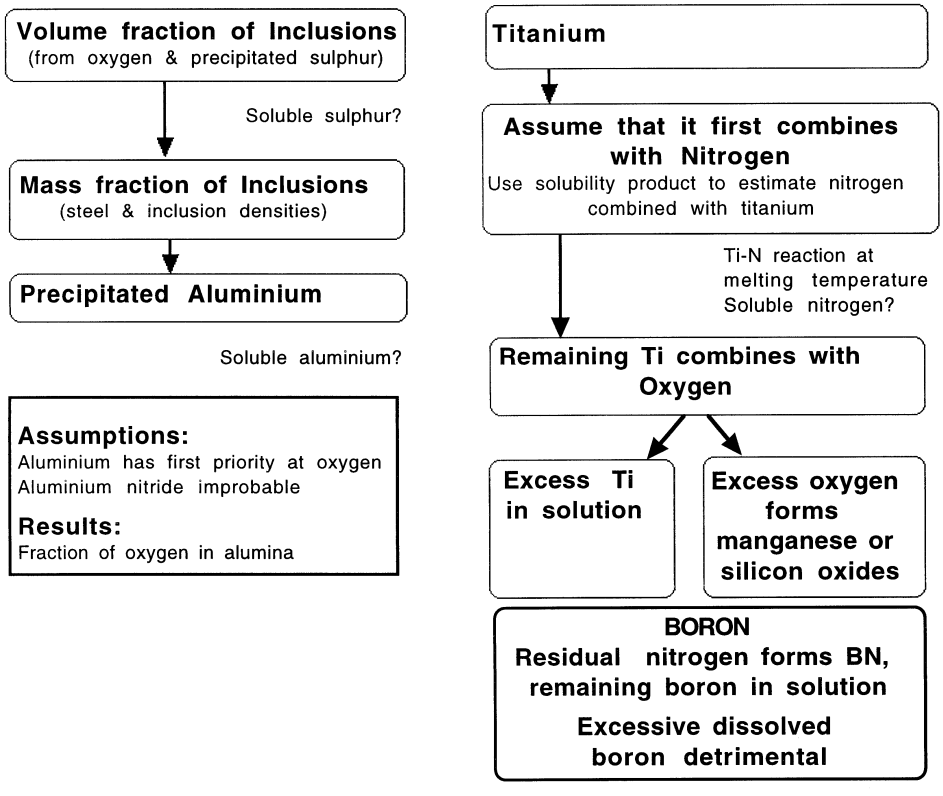

Fig. 10.13 Procedure for the estimation of inclusion microstructure. The assumptions and difficulties associated with the method are placed outside of the main boxes.

[13:36 3/9/01 C:/3B2 Templates/keith/3750 BAINITE.605/3750-010.3d] Ref: 0000 Auth: Title: Chapter 00 Page: 255 237-276

where ρ_S and ρ_I are the steel and inclusion densities, about 7.8 and 4.2 $\mathrm{g\,cm^{-3}}$ respectively. It follows that the concentration of Al in the inclusions is given by:

$$w_{Al}^{I} = \left(w_{Al}^{T} - w_{Al}^{sol}\right)/m_I \tag{10.6}$$

where w_{Al}^{T} and w_{Al}^{sol} represent the total and soluble aluminium concentrations respectively. It is reasonably assumed here that none of the aluminium is in the form of aluminium nitride.

It may be assumed that the titanium reacts first with oxygen, and that any residual titanium can then proceed to combine with nitrogen. In the absence of active oxygen, the titanium nitride can be estimated by calculating the nitrogen in solution using a solubility product (Matsuda and Okumura, 1978):

$$\log\left\{\left[w_{Ti}^{sol}\right]\left[w_{N}^{sol}\right]\right\} = \frac{8000}{T} + 0.32 \tag{10.7}$$

assuming that the concentration of dissolved titanium is known. The temperature for which the calculation is to a good approximation the melting temperature of the steel. The quantity of titanium nitride in the inclusion (w_{Ti}^{I-N}), is then given by:

$$w_{Ti}^{I-N} = A_{Ti}\left(w_{N}^{T} - w_{N}^{sol}\right)/\left(m_I A_N\right) \tag{10.8}$$

where A_i represents the atomic weight of element i. It follows that the titanium in the inclusions, tied up as oxide (w_{Ti}^{I-O}) is given by

$$w_{Ti}^{I-O} = \left(w_{Ti}^{T} - w_{Ti}^{I-N} m_I - w_{Ti}^{sol}\right)/m_I \tag{10.9}$$

This differs from equation 13a of Kluken and Grong, which does not account for the titanium nitride. The sulphur content of the inclusion is similarly given by:

$$w_{S}^{I} = \left(w_{S}^{T} - w_{S}^{sol}\right)/m_I \tag{10.10}$$

Assuming that the sulphur is incorporated in the inclusion as manganese sulphide, the concentration of Mn in the inclusion as MnS is given by

$$w_{Mn}^{I-S} = A_{Mn} w_{S}^{I}/A_S. \tag{10.11}$$

The next step involving the calculation of the SiO_2 and MnO contents of the inclusion requires some assumption about the relative proportions of these two phases.

$$\text{If} \qquad \theta = \text{wt\% } SiO_2/\text{wt\% MnO} \tag{10.12}$$

$$\text{and} \qquad \beta = \frac{\left(\frac{A_{Mn}}{A_O} + 1\right)\theta}{\left(\frac{A_{Si}}{2A_O} + 1\right) + \left(\frac{A_{Mn}}{A_O} + 1\right)\theta} \tag{10.13}$$

$$\text{then} \qquad w_{Si}^{I} = \beta A_{Si}\left(w_O^T - m_I w_O^{I-Al} - m_I w_O^{I-Ti}\right)/(2m_I A_O) \tag{10.14}$$

where w_O^{I-Al} and w_O^{I-Ti} are the concentrations of oxygen in the inclusion, tied up as alumina and titania respectively. It follows that:

$$w_{Mn}^{I-O} = (1-\beta)A_{Mn}\left(w_O^T - m_I w_O^{I-Al} - m_I w_O^{I-Ti}\right)/(m_I A_O) \tag{10.15}$$

These estimates require a knowledge of the dissolved Al, Ti and S concentrations and assume that the oxidation state of the titanium is known. Titanium compounds such as TiN, TiC and TiO have similar lattice parameters and crystal structures and are difficult to distinguish using diffraction. Common microanalytical techniques can readily identify titanium but not the light elements. Even when oxygen can be detected, the stoichiometry is difficult to determine since absorption and other corrections are not known for complex shapes. Lau *et al*. assumed that the Ti is in the form of TiO_2 whereas Kluken and Grong assumed it to be combined as Ti_2O_3. Abson (1987a) on the other hand, assumes that in weld deposits, the titanium oxide is TiO. The major weakness, however, is the method of partitioning oxygen between the different metallic elements. It can for example, be demonstrated that manganese and silicon oxides are found in systems where oxygen is expected to combine completely with Al and Ti. Moreover, the silicon concentration has been known to influence the ability of titanium to combine with oxygen (Lee and Pan, 1992a).

The real picture is evidently complex, but the sequence of reactions should at least determine the microstructure of the inclusions, with the first compounds to precipitate being located at the inclusion core, Fig. 10.14. It is the least reactive elements which should end up at the inclusion surface. Indeed, non-metallic particles in some submerged arc weld deposits have been identified with titanium nitride cores, surrounded by a glassy phase containing manganese, silicon and aluminium oxides, with a thin layer of manganese sulphide partly covering the inclusion surface (Barbaro *et al*., 1988). Similarly, in a weld free from aluminium or titanium, the inclusion core was found to be MnO–SiO_2 whereas the addition of only 40 p.p.m. of aluminium introduced alumina in the core (Es-Souni and Beaven, 1990). On the other hand, both these investigations reported the presence of unspecified titanium compounds over a part of the inclusion surface. It is possible that this reflects an incomplete coverage of the titanium compound core by subsequent phases.

10.4.5 Boron and Hydrogen

Experiments using secondary ion mass spectroscopy have revealed a tendency for boron to form a BH+ complex with hydrogen when both are in solution in steel (Pokhodnya and Shvachko, 1997). A consequence of this is that the mobi-

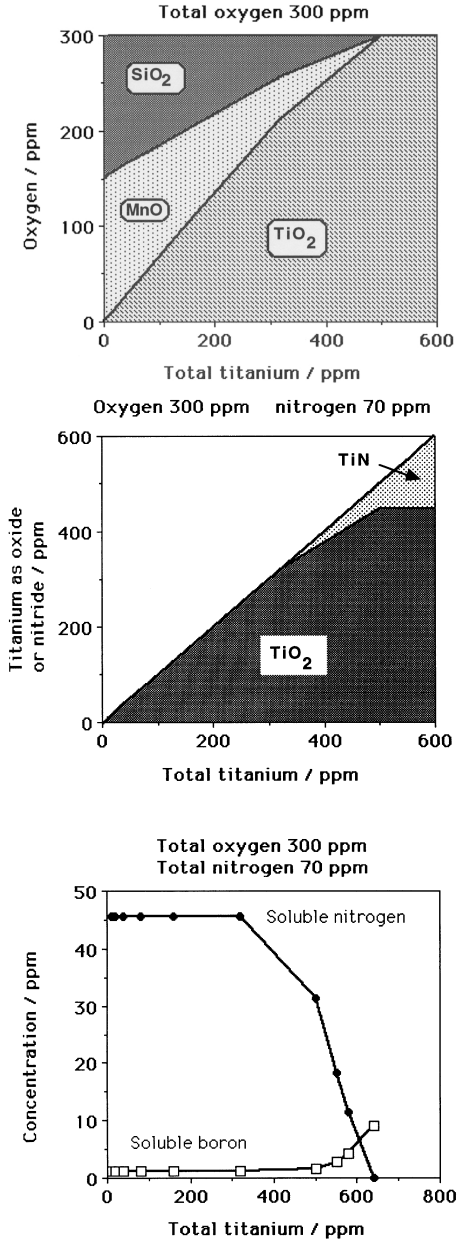

Fig. 10.14 Calculations showing how the components of inclusions in welds change as the chemical composition is altered. Manganese and silicon oxides are progressively replaced by titanium oxide. When the oxygen has reacted completely with titanium, the latter begins to combine with nitrogen and helps to liberate boron.

[13:36 3/9/01 C:/3B2 Templates/keith/3750 BAINITE.605/3750-010.3d] Ref: 0000 Auth: Title: Chapter 00 Page: 258 237-276

lity of both the boron and hydrogen is reduced. Furthermore, more of the hydrogen gets trapped resulting in a strong correlation between the boron and hydrogen concentrations, as shown in Fig. 10.15.

10.4.6 Stereological Effects

There is no doubt that plates of acicular ferrite nucleate on inclusions, although once the process begins, other plates can be stimulated autocatalytically. A one-to-one correspondence between the plates of acicular ferrite and inclusions is therefore not expected. It is difficult to establish the presence of an inclusion in a plate using metallography. By analogy with the procedure used by Chart *et al*. (1975) for aluminium alloys, if the volume of a typical plate of acicular ferrite is taken to be $10^{-16}\,m^3$, and that of a spherical inclusion $4 \times 10^{-20} m^3$, then of all the grains examined, only 7.4% can be expected to display the nucleating particle. When a particle is detected, its intercept on the plane of section will in general be smaller than its diameter. The estimate by Chart *et al*. is strictly valid when the grains of the major phase are spherical, which acicular ferrite plates are not. If the acicular ferrite is approximated as a square plate of side 10 μm and thickness $t = 1$ μm, containing an inclusion of radius $r = 0.2$ μm, the ratio of the mean linear intercepts of the two phases is given by $4r/6t$ (Myers, 1953; Mack, 1956). If every plate contains an inclusion, some 13% will show the nucleating particle in a plane section which is large enough.

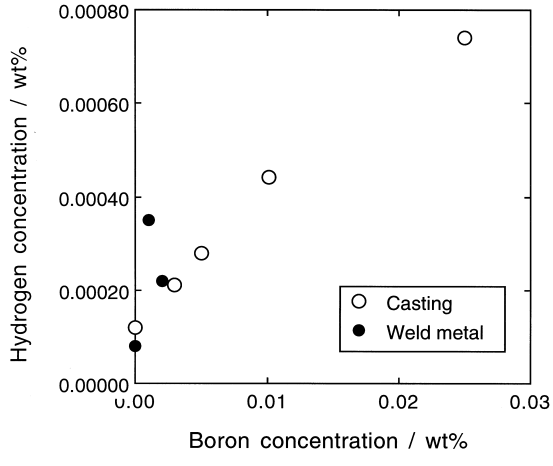

Fig. 10.15 The correlation between the residual hydrogen concentration and the total boron concentration in a series of castings and weld deposits (after Pokhodnya and Shvachko, 1997).

[13:36 3/9/01 C:/3B2 Templates/keith/3750 BAINITE.605/3750-010.3d] Ref: 0000 Auth: Title: Chapter 00 Page: 259 237-276

The estimate assumes that each plate contains just one inclusion, and more importantly, that each observed inclusion is responsible for nucleating the plate in which it is found, i.e. it has not been incorporated accidentally into the plate as a consequence of growth. It is not safe to assume that the observation of a particle in the plate implies that it was responsible for originating the plate when the total fraction of acicular ferrite is large.

An alternative way of establishing the role of autocatalysis is by examining the orientation relationships between adjacent plates in clusters of acicular ferrite plates. The clusters have been found to contain similarly oriented plates with a probability which is larger than random, implying autocatalysis (Yang and Bhadeshia, 1989a).

10.5 Effect of Inclusions on the Austenite Grain Size in Welds

A microstructure with large austenite grains has a better chance of transforming to acicular ferrite because the number density of grain boundary nucleation sites is reduced. It is sometimes assumed that the austenite grain size is determined by Zener pinning by inclusions. This analogy is, however, not justified since the austenite grains form by the *transformation* of δ-ferrite grains which evolve during solidification, whereas Zener pinning deals with the hindrance of grain boundaries during grain growth. The driving force for grain growth typically amounts to just a few Joules per mole, whereas that for transformation from δ-ferrite to austenite increases indefinitely with undercooling below the equilibrium transformation temperature. Pinning of δ/γ interfaces cannot then be effective. A mechanism in which inclusions pin the columnar austenite grain boundaries is also inconsistent with the *shape* of these grains, since the motion of the of the δ/γ interfaces along the steepest temperature gradients is clearly not restricted; if pinning were effective, the austenite grains that evolve should be isotropic.

10.6 Influence of Other Transformation Products

In weld deposits, acicular ferrite is one of the last transformation products to form after the growth of allotriomorphic and Widmanstätten ferrite. As a consequence, it is bound to be influenced by prior transformation products. Indeed, its volume fraction during continuous cooling transformation of such welds can in many cases be estimated simply by calculating the volume fractions of allotriomorphic and Widmanstätten ferrite, and assuming that the remainder of the austenite transforms to acicular ferrite (Bhadeshia *et al.*, 1985). For the same reason, it is found that in wrought alloys with mixed microstruc-

tures, the amount of acicular ferrite decreases with the austenite grain size, as grain boundary nucleated phases such as allotriomorphic ferrite become more dominant (Barbaro *et al*., 1988). The dependence of the volume fraction of acicular ferrite on the austenite grain size becomes less pronounced as the cooling rate (from the austenite phase field) is increased, since at slow cooling rates, much of the austenite is consumed during the higher temperature formation of allotriomorphic ferrite.

This dependence of the acicular ferrite content on the austenite grain size, in a mixed microstructure of acicular ferrite and allotriomorphic ferrite, can for isothermal reaction be expressed precisely using the relationship:

$$\ln\{1-\xi\} \propto S_V \tag{10.16}$$

where ξ is the volume fraction of allotriomorphic ferrite divided its equilibrium volume fraction at the temperature concerned and S_V is the amount of austenite grain surface per unit volume of sample. If a number of reasonable assumptions are made (Bhadeshia *et al*., 1987) the proportionality can be applied to continuous cooling transformation in low-carbon, low-alloy steels, in which case, $(1-\xi)$ is approximately equal to the volume fraction of acicular ferrite, thus relating the latter to the austenite grain size.

An interesting observation reported by Dallum and Olson (1989) is that in samples containing mixtures of allotriomorphic ferrite, Widmanstätten ferrite and acicular ferrite, a relatively small austenite grain size leads to a coarser acicular ferrite microstructure. They attributed this to an reduction in the α_a nucleation rate, caused by some unspecified interaction with the prior transformation products (α and α_w). An alternative explanation could be that with a smaller austenite grain size, the volume fractions of α and α_w that form are correspondingly larger, thereby causing a higher degree of carbon enrichment in the residual austenite and hence a significant reduction in the acicular ferrite nucleation rate. A reduction in the nucleation frequency would then permit the fewer plates to grow to larger dimensions before hard impingement with other plates in the vicinity.

Effects like these are of considerable importance in the development of mixed microstructures, but the coarsening of acicular ferrite without any change in shape *per se* is unlikely to lead to any drastic changes in the strength of weld deposits (Bhadeshia and Svensson, 1989a,b). This is because the mean slip distance in a plate does not change much as the plate becomes larger. Of course, it remains to be demonstrated whether toughness is sensitive to small variations in the size and distribution of acicular ferrite.

10.6.1 Some Specific Effects of Allotriomorphic Ferrite

We now proceed to consider a particular role of allotriomorphic ferrite formation in influencing the development of acicular ferrite in mixed microstructures. The effect is especially prominent in chromium- and molybdenum-containing steels. At relatively high concentrations of chromium (> 1.5 wt%) or molybdenum (> 0.5 wt%), the columnar austenite grains of steel weld deposits transform into bainite instead of acicular ferrite. The bainite is in the form of classical sheaves emanating from the austenite grain surfaces, often with layers of austenite left untransformed between the individual platelets of bainitic ferrite. This is in spite of the presence of nonmetallic inclusions, which usually serve to intragranularly nucleate the plates of acicular ferrite. The effect is probably a consequence of the fact that as the amount of allotriomorphic ferrite decreases with increasing solute concentrations, the austenite grain boundaries are freed to nucleate bainite (Fig. 10.16). The observations of Sneider and Kerr

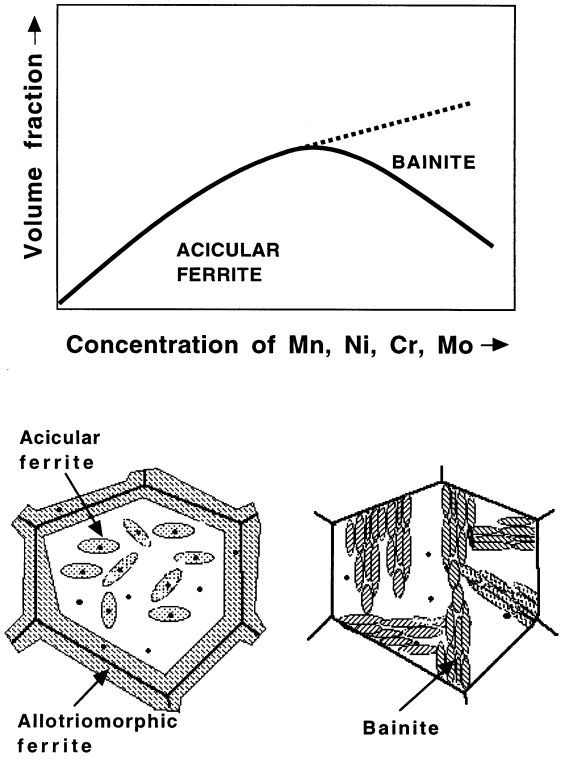

Fig. 10.16 Schematic illustration of the mechanism by which the presence of allotriomorphic ferrite at the austenite grain surfaces induces a transition from a bainitic to acicular ferrite microstructure.

[13:36 3/9/01 C:/3B2 Templates/keith/3750 BAINITE.605/3750-010.3d] Ref: 0000 Auth: Title: Chapter 00 Page: 262 237-276

(1984) could be interpreted to support this conclusion. In welds containing a variety of chromium concentrations, with microstructures which are predominantly acicular ferrite, the amount of bainite increased directly as the volume fraction of allotriomorphic ferrite decreased. In addition, bainite was not found when the allotriomorphic ferrite volume fraction was greater than 0.08, presumably because in their welds, that quantity was sufficient to completely cover the austenite grain surfaces, and prevents the grain boundary nucleation of bainite at a lower transformation temperature.

It may not be necessary to entirely cover the austenite grain surfaces with allotriomorphic ferrite, because the ferrite will tend to form at the most potent nucleation sites, thereby disabling the most active areas of the grain surfaces.

Some interesting quantitative data have also been reported by Evans (1986); he found that as the chromium or molybdenum concentration of low-carbon weld deposits is increased, the amount of allotriomorphic ferrite decreases. The volume fraction of acicular ferrite goes through a maximum as a function of concentration. The volume fraction of the remainder of the microstructure, which is described as 'ferrite with aligned second phase' therefore increases with concentration (Fig. 10.17). This is the terminology used in the welding industry to describe a microstructure in which parallel plates of ferrite are separated by regions of residual phase such as retained austenite. It really refers to packets of parallel plates of Widmanstätten ferrite or to sheaves of

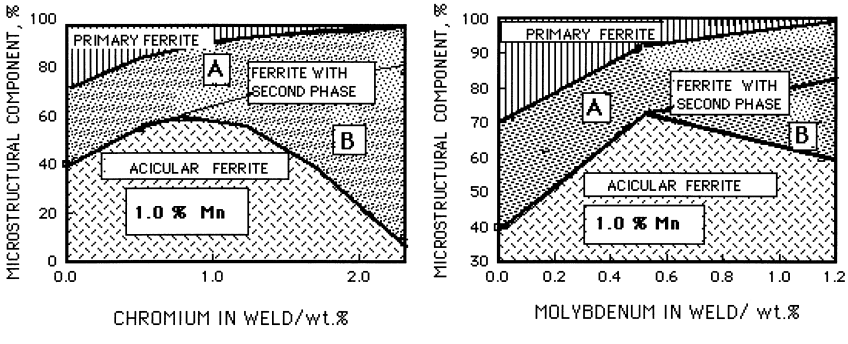

Fig. 10.17 Changes in the as-deposited microstructure of steel welds as a function of chromium or molybdenum concentration (after Evans). Notice that in each case, the fraction of acicular ferrite goes through a maximum as the Cr or Mo concentration increases. The region labelled 'ferrite with aligned second phase' by Evans has been subdivided schematically into regions A and B, to represent the Widmanstätten ferrite and bainite microstructures respectively. The maximum occurs because at large alloy concentrations, acicular ferrite is progressively replaced by austenite grain boundary nucleated bainite.

bainitic ferrite. There is some evidence (Bhadeshia *et al*., 1986b) that in typical welds deposits of the type studied by Evans, the fraction of Widmanstätten ferrite decreases to small values (0.04–0.1) as the chromium or molybdenum concentration increases, so that most of the increase in the volume fraction of the 'ferrite with aligned second phase' can be ascribed to an increase in the volume fraction of bainite (Fig. 10.17). The fact that bainite is obtained when the austenite grain boundaries are free from other transformation products is also consistent with the observation that Fe–2.25Cr–1Mo wt% weld deposits used in the power generation industry are well known to have an almost fully bainitic microstructure (variously referred to as conventional bainite or granular bainite) in the as-deposited condition, with classical sheaves in which the platelets of bainitic ferrite are partially separated by films of retained austenite or martensite (Klueh, 1974b; Wada and Eldis, 1982; Kar and Todd, 1982; Lundin *et al*., 1986; Vitek *et al*., 1986; McGrath *et al*., 1989). The large alloy concentration in this steel prevents the growth of allotriomorphic ferrite under normal heat-treatment conditions.

It appears therefore, that at relatively large concentrations of chromium and/or molybdenum, acicular ferrite is in increasing proportions, replaced by classical bainite, until eventually, the microstructure becomes almost entirely bainitic. This effect cannot be attributed to any drastic changes in the austenite grain structure, nor to the inclusion content of the weld deposits (Babu and Bhadeshia, 1990). It turns out in fact, that the Cr and Mo alloys have highlighted a more general condition associated with welds containing high concentrations of alloying additions. Several cases have been reported in the literature, where a similar transition from an acicular ferrite microstructure to one containing a greater amount of bainite is found to occur as the concentration of elements other than Cr or Mo is increased so that the amount of allotriomorphic ferrite is reduced. Horii *et al*. (1988) found that in a series of low-alloy steel welds, when the manganese or nickel concentrations exceeded about 1.5 and 2.9 wt% respectively, the weld microstructure was found to exhibit significant quantities of bainite. Interestingly, in the case of the nickel-containing steels, the toughness nevertheless improved since nickel in solid solution has a beneficial intrinsic effect on the toughness of iron. It apparently increases the stacking fault energy of body-centred cubic iron; since the dislocations in such iron are three-dimensionally dissociated, the change in stacking fault energy reduces the stress required for plastic flow at low temperatures, relative to that necessary for cleavage fracture (see Leslie, 1982).

To summarise, many experiments have indirectly revealed that the cause for the transition from a predominantly acicular ferrite microstructure to one containing substantial amounts of bainite, may be related to the reduction in the coverage of austenite grain boundaries by layers of allotriomorphic ferrite, as the solute concentration exceeds a certain value (Babu and Bhadeshia, 1990).

Below that concentration, the steel hardenability is low enough to ensure that the austenite grain surfaces are completely covered by uniform layers of allotriomorphic ferrite, thereby rendering them useless for bainite nucleation, and consequently allowing the development of acicular ferrite by intragranular transformation. As the concentration of austenite stabilising elements is increased, some of the austenite grain surface is left bare and becomes available for the nucleation of bainite sheaves as soon as the temperature falls within the bainite transformation range.

These ideas have been verified directly in experiments on Cr-containing steels, which demonstrated that the microstructure can be changed from bainite to acicular ferrite simply by introducing thin layers of allotriomorphic ferrite at the austenite grain surfaces (Fig. 10.18). It appears that the allotriomorphic ferrite/austenite boundaries, even when the α/γ orientation is appropriate, cannot develop into bainite because the adjacent austenite is enriched in carbon, to an extent which drastically reduces its bainite start temperature. A transformation-free zone is therefore found ahead of the allotriomorphic ferrite/austenite interfaces.

10.7 Lower Acicular Ferrite

We have seen that acicular ferrite and bainite seem to have similar transformation mechanisms. The microstructures might differ in detail because bainite sheaves grow as a series of parallel platelets emanating from austenite grain *surfaces*, whereas acicular ferrite platelets nucleate intragranularly at *point* sites so that parallel formations of plates cannot develop. Some of the similarities between bainite and acicular ferrite are:

1. They both exhibit the invariant-plane strain shape deformations with large shear components, during growth. Consequently, the growth of a plate of acicular ferrite or bainite is confined to a single austenite grain (i.e. it is hindered by a grain boundary) since the coordinated movement of atoms implied by the shape change cannot in general be sustained across a border between grains in different crystallographic orientations. A further implication is that plates of acicular ferrite, like bainite, *always* have an orientation relationship with the parent phase, which is within the Bain region. This is not necessarily the case when the transformation occurs by a reconstructive mechanism.
2. There is no substitutional solute partitioning during the growth of either bainite or acicular ferrite (Strangwood, 1987; Chandrasekharaiah *et al.*, 1994).
3. Both reactions stop when the austenite carbon concentration reaches a value where it becomes thermodynamically impossible to achieve

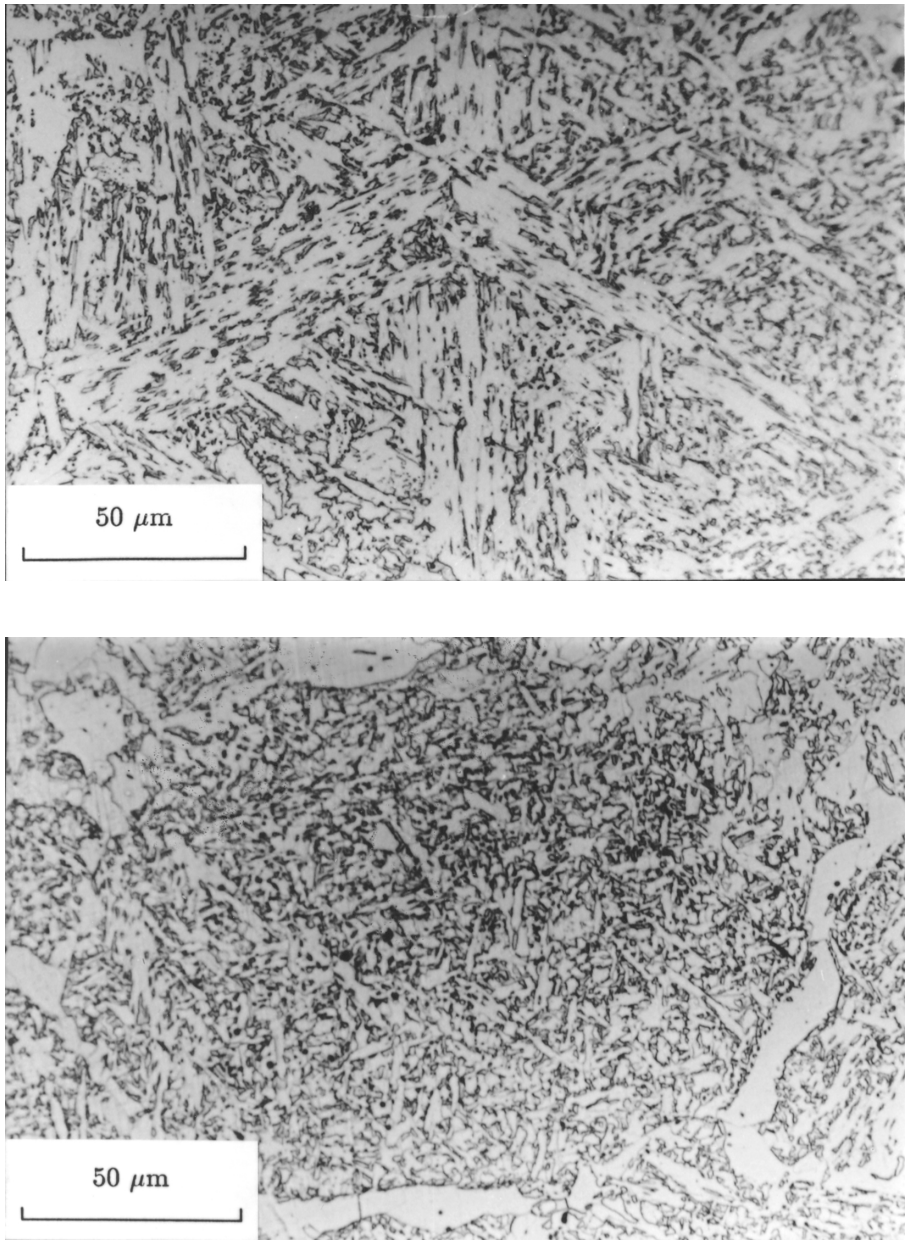

Fig. 10.18 The change from a bainitic microstructure (a) to one which is predominantly acicular ferrite (b), induced by the introduction of a thin layer of allotriomorphic ferrite at the austenite grain surfaces. Both the acicular ferrite and bainite were otherwise obtained by isothermal transformation under identical conditions (after Babu and Bhadeshia, 1990).

diffusionless growth (Yang and Bhadeshia, 1987b; Strangwood and Bhadeshia, 1987a). Any redistribution of carbon from the supersaturated ferrite plates occurs after growth. Growth is thus diffusionless, but is followed immediately afterwards by the rejection of carbon into the residual austenite.

4. Acicular ferrite only forms below the bainite-start temperature.
5. There is a large and predictable hysteresis in the temperature at which austenite formation begins from a mixed microstructure of acicular ferrite and austenite, or bainite and austenite (Yang and Bhadeshia, 1987a).
6. The removal of inclusions from a weld deposit, without changing any other feature, causes a change in the microstructure from acicular ferrite to bainite (Harrison and Farrar, 1981).
7. An increase in the number density of austenite grain surface nucleation sites (relative to intragranular sites) causes a transition from acicular ferrite to bainite (Yang and Bhadeshia, 1987a).
8. The elimination of austenite grain surfaces by decoration with inert allotriomorphic ferrite leads to a transition from a bainitic to an acicular ferritic microstructure (Babu and Bhadeshia, 1990).

These and other similarities emphasise the point that bainite and acicular ferrite have the same growth mechanisms. There is one anomaly. Like conventional lower bainite in wrought steels, there ought to exist a *lower* acicular ferrite microstructure, in which the intragranularly nucleated plates of α_a contain plates of cementite inclined at an angle of about 60° to the habit plane (Bhadeshia & Christian, 1990). The transition from upper to lower bainite occurs when the partitioning of carbon from supersaturated bainitic ferrite into austenite becomes slow compared with the precipitation of carbides in the ferrite, Fig. 7.1 (Hehemann, 1970; Takahashi and Bhadeshia, 1990). Consequently, if the carbon concentration of a steel weld is increased sufficiently (Fig. 7.2), then for similar welding conditions, the microstructure should undergo a transition from acicular ferrite to lower acicular ferrite. An experiment designed to test this, using an exceptionally high carbon weld, has detected lower acicular ferrite (Sugden & Bhadeshia, 1989b), supporting the conclusion that acicular ferrite is simply intragranularly nucleated bainite (Fig. 10.19). Lower acicular ferrite is only found when the weld carbon concentration is large enough to permit the precipitation of carbides from the acicular ferrite, before much of the carbon can partition into the residual austenite. This means that in reality, lower acicular ferrite is unlikely to be of technological significance in welds which necessarily have low carbon equivalents. On the other hand, lower acicular ferrite has been detected in a laser welded high-carbon steel (Hall, 1990).

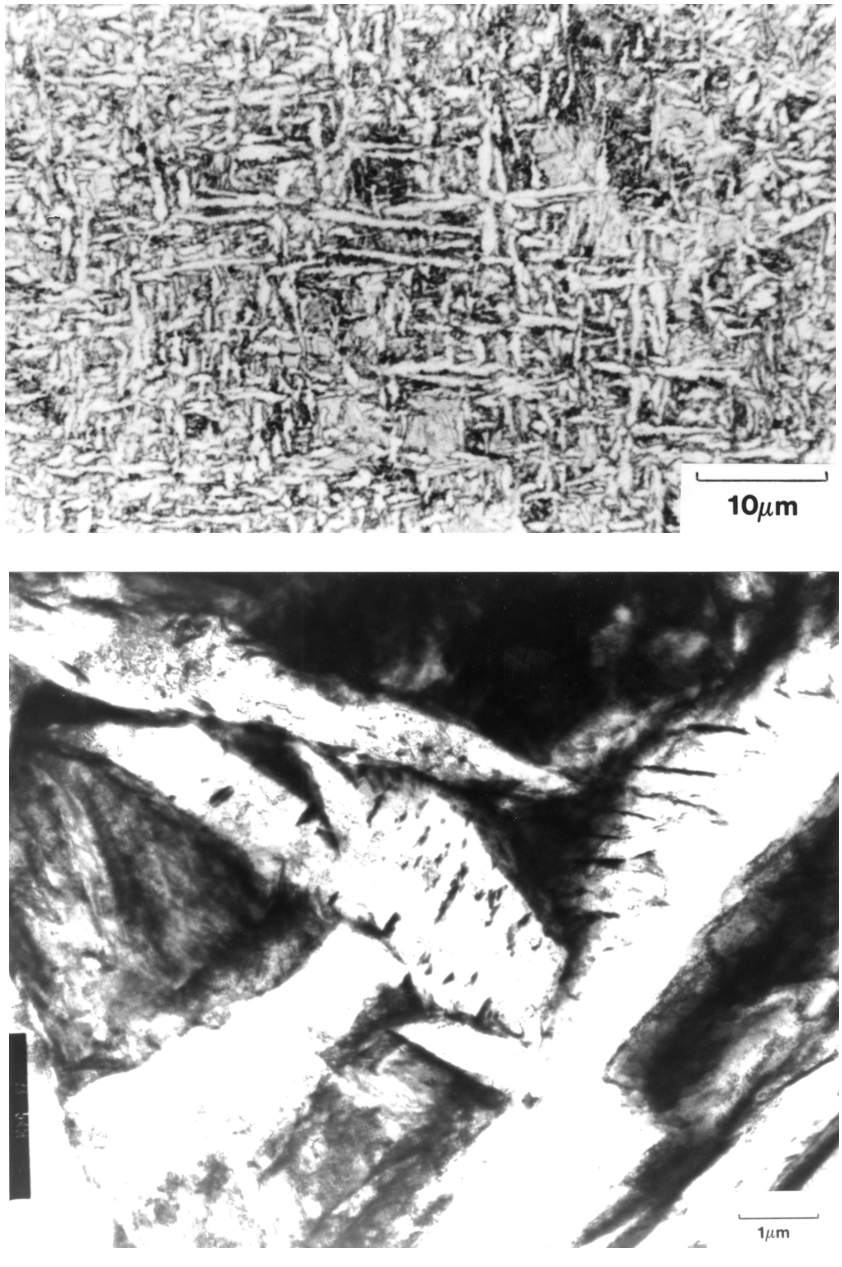

Fig. 10.19 (a) Light micrograph of lower acicular ferrite in an experimental high-carbon steel weld deposit (Sugden and Bhadeshia, 1989b). (b) Corresponding transmission electron micrograph illustrating the carbide particles in the acicular ferrite, in the single crystallographic variant typical of lower bainite in conventional microstructures.

10.8 Stress-Affected Acicular Ferrite

Welded fabrications are prone to the development of residual stresses whose magnitudes may approach the yield stress. This may have consequences on the development of the acicular ferrite microstructure during the cooling of the weld to ambient temperature. Dallum and Olson (1989) have shown that stress has little influence on the overall volume fraction of acicular ferrite. Nevertheless, an externally applied stress accelerates transformation and alters the morphology of acicular ferrite as shown in Fig. 10.20. This is not surprising given the displacive character of the transformation.

10.9 Effect of Strain on the Acicular Ferrite Transformation

The distinguishing feature of acicular ferrite is that it must nucleate intragranularly on inclusions. The amount of acicular ferrite is reduced if the number density of grain boundary nucleation sites is increased relative to the number density of inclusions.

The effect of deforming austenite prior to its transformation is to increase the nucleation potency and number density of the austenite grain boundaries. This is not helpful in promoting acicular ferrite. This is why the thermomechanical processing of austenite prior to its transformation discourages the formation of acicular ferrite (Shim *et al.*, 2000).

10.10 Inoculated Acicular Ferrite Steels

We have seen that acicular ferrite in weld deposits is intragranularly nucleated bainite. An acicular ferrite microstructure appears different from that of bainite because its plates nucleate from point sites, the non-metallic inclusions present in the steel. Adjacent plates of acicular ferrite tend to radiate in many directions from each nucleation site. A propagating crack is therefore frequently deflected as it encounters plates in different crystallographic orientations, leading to an improvement in the toughness.

Bainite and acicular ferrite can be obtained under identical isothermal transformation conditions in the same inclusion-rich steel. Bainite dominates when the austenite grain size is small, i.e. the number density of grain boundary nucleation sites is large relative to the number density of inclusions. Conversely, acicular ferrite is not easily obtained in clean steels.

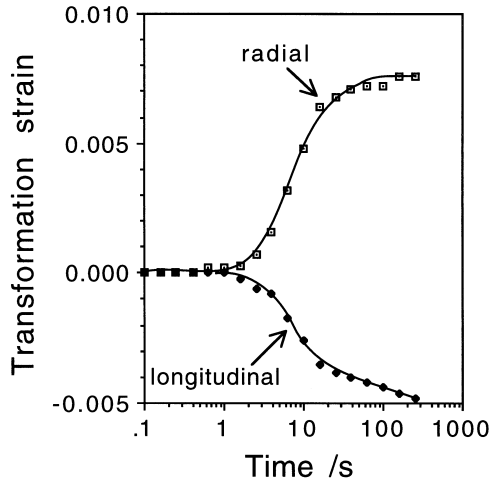

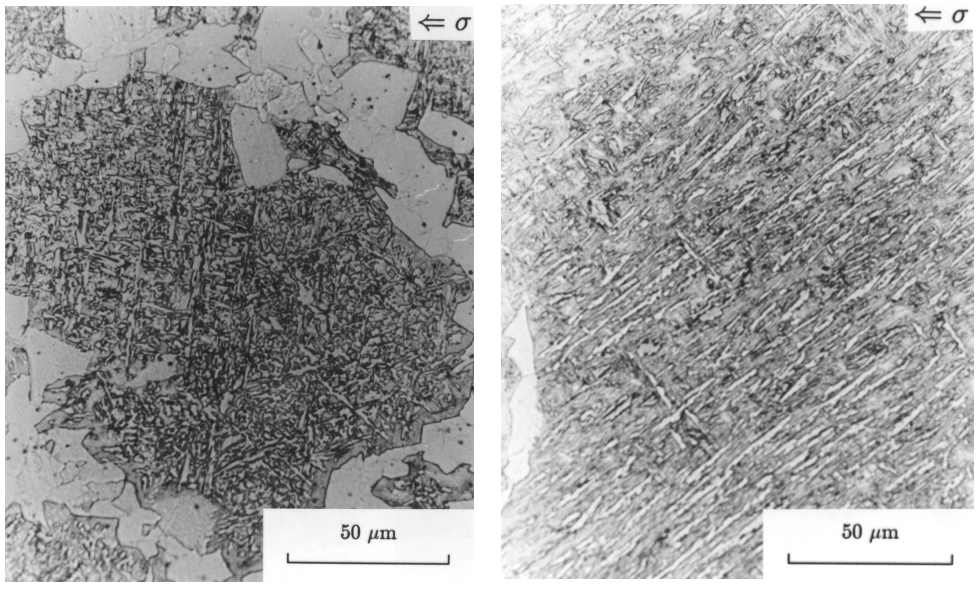

Fig. 10.20 (a) Dilatometric data monitored along orthogonal directions, showing the displacive character of the acicular ferrite reaction, and the acceleration of transformation by the applied stress. (b) The microstructure obtained in the absence of stress. (c) The aligned microstructure generated by the formation only of those acicular ferrite variants which are favoured by the applied stress. The transformation conditions for (b) and (c) are otherwise identical (after Babu).

10.10.1 Structural Steel

It is more than ten years now since the invention of steels with deliberate additions of oxide particles to induce the formation of acicular ferrite and hence to achieve better toughness (Nishioka and Tamehiro, 1988).† More than 100,000 tonnes of these inoculated steels have been marketed for applications in the offshore oil and gas industries, and for constructions in hostile, deep and cold environments. Steels destined for the Arctic regions must have adequate toughness at temperatures as low as $-80\,^{\circ}C$. In some cases, the steels have to be amenable to high heat-input welding ($4\,kJ\,mm^{-1}$) typical in ship construction. It follows that the designed microstructure must be left unchanged by any heat originating from the welding process. Regions of the heat-affected zone which become austenitic must transform back into an appropriate microstructure which is tough.

Inoculated steels have many advantages in this context. The coarse austenite grain structures found in the heat-affected zone adjacent to the fusion boundary favour the development of acicular ferrite plates on the titanium oxides and nitrides.

A typical composition of an inoculated structural steel is Fe–0.08C–0.2Si–1.4Mn–0.012Ti–0.002Al–0.002N wt%. Small concentrations of boron may be added to discourage grain boundary allotriomorphic ferrite and to fix free nitrogen which reduces toughness via a strain hardening mechanism.

The oxide particles effective in stimulating nucleation are about 2 μm in size. They are introduced during steel making by controlling the deoxidation practice. Each particle is generally a mixture of many compounds [MnS, Al_2O_3, (Mn,Si)O etc.] but the key phase responsible for the nucleation of ferrite is Ti_2O_3, although the published experimental evidence is rather limited (Homma *et al*., 1987; Nishioka and Tamehiro, 1998).

Aluminium has a strong affinity for oxygen; its concentration must be kept below about 30 p.p.m. to allow titanium to combine with oxygen. The fraction of the total oxide content which is due to titanium decreases as the aluminium concentration increases (Fig. 10.21).

Aluminium dissolved in austenite promotes Widmanstätten ferrite at the expense of acicular ferrite, the fraction of which decreases sharply at concentrations greater than about 70 p.p.m. (Fig. 10.22a). The mechanism of this effect is unknown and the concentration of dissolved aluminium is difficult to

†Prior to the advent of the oxide-inoculated wrought steels, high-strength low-alloy steels were sometimes called 'acicular ferrite HSLA' steels (Krishnadev and Ghosh, 1979). However, their microstructure consisted of parallel, heavily dislocated laths in identical crystallographic orientation. It is modern practice to restrict the term acicular ferrite to more chaotic microstructures.

[13:36 3/9/01 C:/3B2 Templates/keith/3750 BAINITE.605/3750-010.3d] Ref: 0000 Auth: Title: Chapter 00 Page: 271 237-276

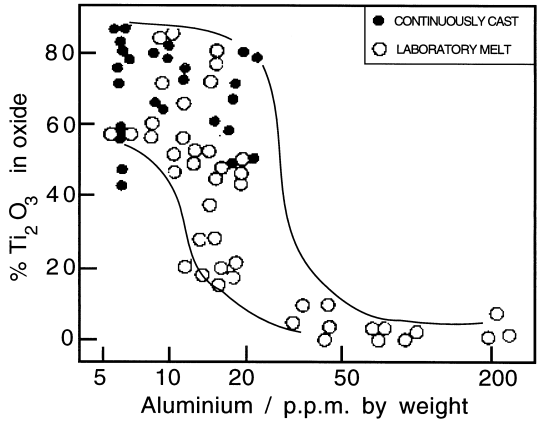

Fig. 10.21 The effect of aluminium concentration on the proportion of Ti_2O_3 in the total oxide content of the steel (Chijiiwa *et al*., 1988).

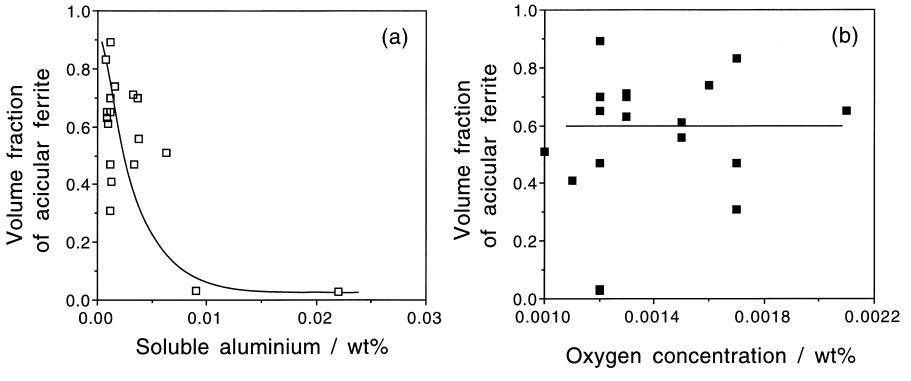

Fig. 10.22 (a) The volume fraction of acicular ferrite as a function of the soluble aluminium concentration; (b) the volume fraction of acicular ferrite as a function of the total oxygen concentration (data from Imagumbai *et al*., 1985).

control in practice. There is little correlation between the total aluminium concentration and that in solution (Thewlis, 1989a,b).

The effect of inclusions in promoting acicular ferrite saturates at about 120 p.p.m. of oxygen (Fig. 10.22b). The oxide content of the steel should be kept to the minimum consistent with the development of acicular ferrite, because any excess contributes towards the initiation of fracture. This is why inoculated steel contains the same amount of oxygen as a fully killed steel; it is the nature of the oxide that is more important than the total concentration of oxygen (Imagumbai *et al*., 1985).

The nitrogen concentration of inoculated steels must be controlled to avoid the formation of TiN which is not as effective as the oxide in stimulating intragranular nucleation. TiN is also not as stable as the oxide and tends to dissolve in the region of the heat-affected zone adjacent to the fusion boundary of a weld.

The design of inoculated steels includes a consideration of hardenability since phases such as allotriomorphic ferrite and Widmanstätten ferrite must be avoided. This ensures that there is sufficient untransformed austenite available for conversion into acicular ferrite. The hardenability can be enhanced by the careful use of microalloying elements such as Nb, Mo and B, thereby minimising the carbon equivalent of the steel. The silicon concentration should be kept below about 0.2 wt% to avoid large oxide particles.

10.10.2 Acicular Ferrite Forging Steels

Forging steels contain a high carbon concentration and hence are not welded. Titanium nitride can therefore be used to produce an acicular ferrite microstructure instead of the more usual mixture of ferrite and pearlite (Linaza *et al.*, 1993). The heat-treatment temperatures are never high enough to take the nitride into solution.

The steels listed in Table 10.4 under normal conditions have the microstructure illustrated in Fig. 10.23a, consisting mainly of pearlite and a small quantity of allotriomorphic ferrite. The same steel, when cooled rapidly transforms to acicular ferrite rather than bainite (Fig. 10.23b,c) because the titanium nitride particles present in the austenite provide abundant sites for intragranular nucleation. The toughness improves but the change is not large at comparable

Table 10.4 Chemical compositions (wt%) and representative mechanical properties of some titanium alloyed forging steels (Linza *et al.*, 1993).

Alloy	C	Mn	Si	V	Al	Ti	N
Ti–V	0.37	1.45	0.6	0.11	0.024	0.015	0.0162
Ti	0.35	1.56	0.33	–	0.027	0.028	0.0089

Alloy	Microstructure	Yield Strength/MPa	K_{IC}/MPa $m^{\frac{1}{2}}$
Ti–V	Acicular ferrite	560–666	133–155
Ti–V	Ferrite & Pearlite	590–650	134–139
Ti	Acicular ferrite	519	169–176
Ti	Ferrite & Pearlite	440	162–169

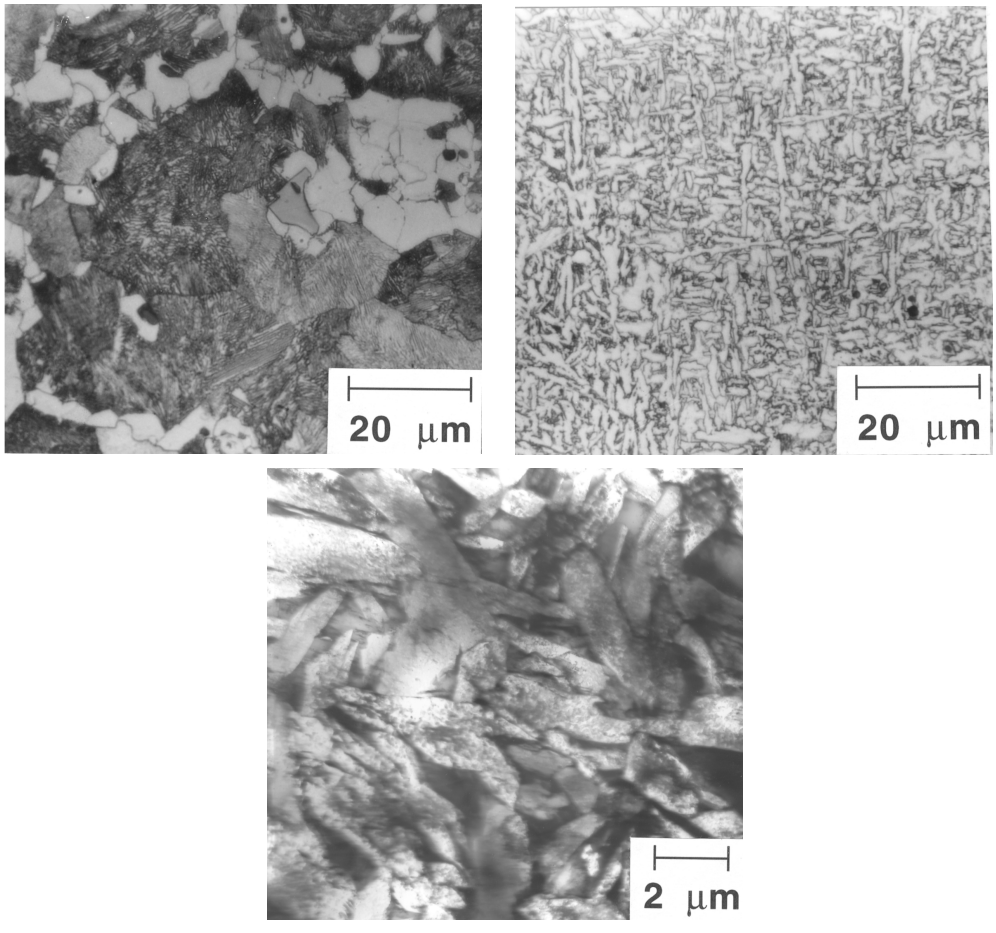

Fig. 10.23 The microstructures of a Ti–V forging steel: (a) optical micrograph showing a mixture of ferrite and pearlite; (b) optical micrograph showing the acicular ferrite microstructure; (c) transmission electron micrograph showing the acicular ferrite microstructure.

yield strength (Table 10.4). This is because some of the TiN particles can be coarse, greater than 2 μm. They are also brittle and hence act to initiate cracks (Rodriguez-Ibabe, 1998).

10.10.3 Steelmaking Technology for Inoculated Alloys

The details of the manufacturing practice for inoculated steels have not been published but the aim is to incorporate titanium oxide (Ti_2O_3) rather than TiN

which is less stable at high temperatures. The steelmaking involves deoxidation with titanium, whilst avoiding other strong deoxidisers such as Al, Ca or the rare earth elements. The oxygen concentration in the molten steel should be between 60 and 120 p.p.m., depending on application. High toughness levels demand a small inclusion (and hence oxygen) content. The steel must otherwise be clean with a minimal concentration of sulphur.

The active inclusions form in the melt or during the solidification stage (Pan and Lee, 1994). The titanium oxide might be added as powder into the melt, or during the casting stage (Ohno *et al*., 1985). However, the oxide then tends to cluster making the distribution of particles uneven. Alternatively, elemental titanium or ferro-titanium may be added to the melt or casting (Nishioka and Tamehiro, 1988; Chijiiwa *et al*., 1988). The titanium then combines with any dissolved oxygen. With this second method, the steel must not be aluminium killed because alumina then forms in preference to titanium oxides, as illustrated in Fig. 10.20. Aluminium-free molten steel is therefore titanium-killed in order to produce an inoculated alloy (Lee and Pan, 1991a, 1991b, 1992, 1993).

10.11 Summary

It is ironic that bainite, when it was first discovered, was called *acicular ferrite* by Davenport and Bain (1930). The terms acicular ferrite and bainite were often used interchangeably for many years after 1930 (see for example, Bailey, 1954). There is good evidence that the microstructure which we now call acicular ferrite, consists simply of intragranularly nucleated bainite. Conventional bainite grows in the form of sheaves of parallel plates which nucleate at austenite grain *surfaces*. By contrast, acicular ferrite plates emanate from *point* nucleation sites and hence grow in many different directions; the development of a sheaf microstructure is prevented by impingement between plates which have nucleated from adjacent inclusions.

The transformation has otherwise been verified to show all the characteristics of the bainite reaction: the incomplete reaction phenomenon, the absence of substitutional solute partitioning during transformation, an invariant-plane strain shape deformation accompanying growth, a large dislocation density, a reproducible orientation relationship within the Bain region, the lower acicular ferrite etc.

Any factor which increases the number density or potency of intragranular nucleation sites at the expense of austenite grain boundary sites favours a transition from a bainitic to an acicular ferrite microstructure. The transition can in practice be obtained by increasing the austenite grain size, by decorating the grain boundaries with thin, inactive layers of allotriomorphic ferrite, by increasing the inclusion content or by rendering the boundaries impotent with elements like boron. It is well understood that these microstructural factors can

only be useful if enough austenite is left untransformed for the development of acicular ferrite – the grain boundary nucleated phases must therefore be kept to a minimum).

[13:36 3/9/01 C:/3B2 Templates/keith/3750 BAINITE.605/3750-010.3d] Ref: 0000 Auth: Title: Chapter 00 Page: 276 237-276